Ann. For. Res. 66(1): 3070-3091, 2023
ISSN: 18448135, 20652445
ANNALS OF FOREST RESEARCH
www.e-afr.org

LANDSLIDE SUSCEPTIBILITY ASSESSMENT FOR ILAM PROVINCE IN IRAN, BY USING MCDM AND GIS TECHNIQUES

Yaser A. Nanehkaran[1], Zhu Licai[1*], Junde Chen[2,3] and Mohammad Azarafza[4]
[1]School of Information Engineering, Yancheng Teachers University, Yancheng 224002, Jiangsu, China
[2]Dale and Sarah Ann Fowler School of Engineering, Chapman University, Orange, CA 92866, USA
[3]Department of Electronic Commerce, Xiangtan University, Xiangtan 411105, Hunan, China
[4]Geotechnical Unit, Faculty of Civil Engineering, University of Tabriz, Tabriz 5166616471, Iran
Corresponding Author: Zhu Licai, School of Information Engineering, Yancheng Teachers University, Yancheng 224002, Jiangsu, China, E-mail: zhulc01@yctu.edu.cn

1. Abstract
Landslides are one of the well-known geological hazards that responsible for extensive damages for infrastructures, roads, facilities, and interference in the general social life of humans. To avoid such catastrophic destructions, the landslide susceptibility assessment must be done. The presented study attempted to provide a landslide susceptibility analysis for Ilam province located in western part of Iran. After a comprehensive field and remote-sensing investigations, fifteen landslide triggering factors are detected for this study which classified as geomorphology, geological, climatological, seismical, and human works major groups. Multi-Criteria Decision-Making (MCDM) model used to rank the triggering factors were prepared to enter in the Geographical Information System (GIS) environment. Totally 10 historical landslides that extracted from literatures was used as ground validation for susceptibility assessments. The results of the susceptibility mapping are categorised into five susceptibility class included very low (12.5%), low (19.21%), moderate (25.49%), high (27.27%), and very high (15.53%). According to the results of the susceptibility assessment for the studied region, it appeared that the most area is in moderate to high risk regarding landslides occurrence. But the northwest part of the province is located in very high-risk zone. So, considering the results, decision-makers should conduct relevant investigations on landslide before planning or developments in high-risk areas at Ilam province.

2. Keywords: Landslides; Susceptibility analysis; MCDM; GIS; Ilam province

3. Introduction
Landslide is one of the well-known geological hazards which is lead different scale disaster that occur in mountainous terrains (Swetha & Gopinath 2020, Sur et al. 2020, Jam et al. 2021, Roy et al. 2022). Landslides caused various damages on infostructures, roads, railways, facilities, cities, and residential areas (Mousavi et al. 2022). These damages mostly associated with human or animal casualties (Zêzere et al. 2017, Chen et al. 2018). The landslides are usually identified as

various geomaterials movement to a slope down as a complex process that is influenced by various tiggering factors such as slope angle, elevation, hydrographic parameters, river/drainage network density or distance from rivers, lithology, soil, land-use/land-cover, distance from faults, etc. (Sahin et al. 2020, Bahrami et al. 2021). In particular, landslides are a permanent geohazard in residential areas where buildings are located on/near slopes or faults which is known as suitable regions for land-sliding or slope failures. The result of such actions is frequent damage on ground and underground structures, engineering networks or agricultural and forest lands which is lead to land-losing event (Azarafza et al. 2021, Nanehkaran et al. 2021, Nikoobakht et al. 2022). All over the world, landslides are considered an important geohazard, which viewed as the second-most noteworthy geo-logical disasters as identified by the United Nations Development Program (Azarafza et al. 2018, Froude & Petley, 2018; Bragagnolo et al. 2020). For landslide disaster mitigation and management, assessment of landslide prone areas is critical (Hong et al. 2016).

Some studies show that landslide hazards become more common over time due to population growth and climate change (Froude & Petley 2018). To investigate hazardous areas regarding the landslides, a set of regulatory factors that known ‘triggering factors’ which responsible for imminent failures in ground must be identified. These triggering factors provide appropriate areas for occurrence of landslides (Khalil et al. 2022). The occurred landslides under influence of triggering factors regardless of the scale or mechanism of failures, causes destructions were properly identified by landslide susceptibility assessments (Maqsoom et al. 2021, Aslam et al. 2022). Therefore, it is inevitable to know and analyse landslide susceptibility for different regions, especially sensitive areas (Santacana et al. 2003). Landslide susceptibility can be used as principle for early warning and ground preparation which provide precise determination of high-risk and low-risk areas in terms of landslides. Landslide susceptibility also can be used to identify the hazardous regions regarding red areas for the construction or urban developments (Yamusa et al. 2022).

There are several procedures that leads to provide landslide susceptibility maps which can be classified in qualitative and quantitative approaches. Various researchers widely used qualitative methods until the late 1970s. Qualitative techniques measure each landslide-causing factor, based on the expertise of researchers, these methods have been widely used to evaluate landslide-prone areas. But later, the quantitative method became the centre of attentions. deterministic, probabilistic, statistic, geostatistic, likehood and inventory, and intelligent methods is the common procedures that used by the professionals to prepare a hazard zonation maps (Youssef et al. 2015, Tsangaratos et al. 2017, Aslam et al. 2022). In the meantime, the decision-based methods have considered more capable to rank the triggering factors and understand the degree of influence of each factor on the landslide’s occurrence is estimated. Also, the models like Multi-Criteria Decision-Making (MCDM) can be properly adopted with Geographical Information System (GIS) environment.

Rozos et al. (2010) used integrated technique of Analytical Hierarchical Process (AHP) and Geographic Information System (GIS) to create a landslide susceptibility map for northeast part of Achaia prefecture (Greek) which is consist of Neogene deposits. The authors used AHP to generate the influencing factors layers and used in GIS to get zonation map regarding landslide occurrence. Akgun & Türk (2010) used multicriteria decision analysis based on MCDM to develop landslide susceptibility assessment for Ayvalik region (Western Turkey). Researchers used weight values of triggering factors to prepare information layers in GIS. Mohammady et al. (2010) attempted to use AHP model for prioritization of landslide triggering factors in Haraz watershed. Yalcin et al. (2011) utilized a comparative analysis for understanding a capability of various statistical procedures and hierarchy process for susceptibility mapping of landslides in Trabzon, Turkey. As results it is appeared that using MCDM models provide reliable results. Kritikos & Davies (2011) applied GIS-based multi-criteria decision analysis in landslide susceptibility mapping for northern part of Evia Island (Greece). The scholars used several triggering factors to identify the high-risk area that selected based on remote-sensing and ground survey results. Khezri (2011) used same procedure for susceptibility mapping in Zab basin in Iran. Pourghasemi et al. (2012), Moradi et al. (2012), and Kayastha et al. (2013) used AHP-based multi-criteria decision models for assessment of probability of landslide occurrence for specific case studies which indicated that the MCDM models has good performance for susceptibility mapping with multiple triggering factors applications. Roodposhti et al. (2014), Himan et al. (2014), and Mansouri Daneshvar (2014) provide various decision-based models for landslide susceptibility analysis in Iran for different case studies. Youssef (2015) used three techniques including AHP for landslide susceptibility analysis of the Ar-Rayth area in Saudi Arabia.

Myronidis et al. (2016), Kumar & Anbalagan (2016) utilized AHP and MCDM procedures to provide hazard zonation maps for landslide by considering weighted multi-criteria matrix systems. The results indicated that using AHP models provide accurate information regarding landslides prone areas. Abedini et al. (2017), Pourghasemi & Rossi (2017), Abedini & Tulabi (2018) attempted to use MCDM as main method to investigate the landslides susceptibility and probability for Kurdistan (Bijar city), Lorestan, & Mazandarn provinces. Mandal and Mandal (2018) used AHP and MCDM for investigate susceptibility assessment of landslides at Lish river basin of eastern Darjeeling Himalaya, India. El-Jazouli et al. (2019), Nguyen and Liu (2019), He et al. (2019) applied AHP-based weighted multi-criteria method to assessment the landslides occurrence probabilities for different cases studies. As results, it is appeared that the MCDM and AHP procedures are received high attention form the researchers worldwide. Sur et al. (2020), Panchal & Shrivastava (2020), and Huang et al. (2020) used AHP for the same purposes to extract the landslide prone-area for their case studies. Bahrami et al. (2021), Devara et al. (2021), Cengiz & Ercanoglu (2022), Das et al. (2022) are used AHP and MCDM procedures to develop new weighted multi-task decision making systems that used in landslide susceptibility and priories the triggering factors which leads to estimate the coefficient of efficacy for each factor. So, it can be coupled with other procedures like fuzzy logic.

As results, using MCDM is one of the accepted methodologies in landslide susceptibility mapping which is provide reliable information about the landslide prone-area and hazard-risk suitability regions. The presented study used the MCDM and AHP-based framework to estimate the landslide susceptibility conditions under multiple triggering factors that leads to provide hazard-risk zonation map for studied province. With the potential to speed up the multi-task analysis, MCDM provides a useful method for obtaining an initial linear approximation of this unexpressed utility function. Using the consistency measure to improve decision maker learning is one more advantage. In this instance, MCDM is capable of resolving multiple or ultimate problems or goals, presenting the most suitable solutions as alternatives, and providing a rational framework for making the right decisions by skillfully quantifying all of the criteria and alternatives that can link all of the key components required to achieve the overall goal.

The objective of this research work is to generate an updated landslide susceptibility map for Ilam Province (Iran) by using AHP multi-criteria decision analysis model. In order to accomplish this goal, the MCDM-based method is initially validated with landslide points obtained from Geological Survey and Mineral Exploration of Iran (GSI) that correspond to identify zones that are susceptible to landslides' occurrence. To highlight the efficacy of the used method, multiple triggering factors (15 different variables) was used in decision process.

4. Studied Case

Ilam Province is in the western part of Iran and covers about 20,164.11 km^2. The province is one of the bordered regions which sharing 425 km of the border with Iraq. Ilam was limited with Kermanshah (north), Lorestan (east), and Khuzestan (south) Provinces. Figure 1 is showing the location map of the studied province. Ilam province is situated at the southwestern edge of Zagros Mountains and right at the transition between the Arabian and the Iranian plateaus. Because of this, it is divided into two distinct natural areas; the northern and eastern parts are mountainous, whereas the southwest is covered with low plains that extend to the Iraqi and Khuzestan borders. The most prominent mountain in Ilam province is Kabir Kouh, which is in the eastern part of the province, stretching 160 km from near Pol-e Zal in the southeast to Mishkhas village near Ilam city in the northwest. The highest point in province, Kan Seifi peak with 2,775 m above sea level, is part of Kabir Kouh range. The mountains in the north and east are mostly parallel, running in the northwest–southeast direction. These mountains are separated by plains and rolling hills that are mostly used to grow crops and orchards by settlers (Aghanabati 2009).

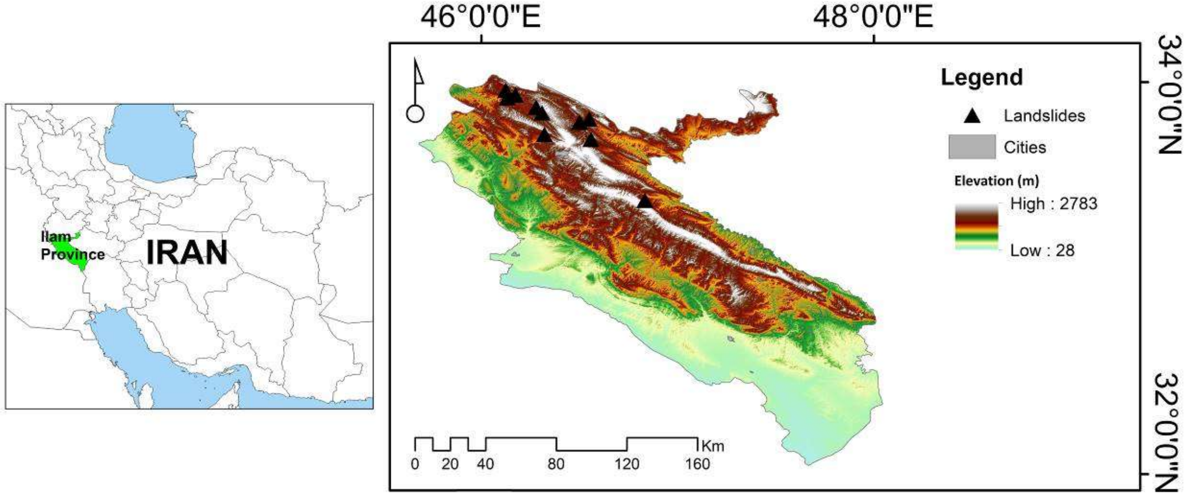

Figure 1: Location of the Ilam province in Iran.

Contrary to the north, the south and south-western part of the province is covered with low-lying plains with elevation varying between 50 to 300 m above sea level. Despite receiving little precipitation, large areas of these lowlands, notably Dehloran, Musian and Dasht Abbas, are cultivated owing to a combination of factors such as rivers flowing from the mountains to the east, dams, and irrigation networks (Aghanabati 2009). Because of the terrain, the permanent and seasonal rivers and stream that originate from Ilam highlands either fall into Seymareh, such as Chardavol, Garab, Seekan, Darreh Shahr and Majeen rivers; or, flow westward toward the low lands and into Iraq and Khuzestan, such as Ghanghir, Ghodar-Khosh, Kanjan-Cham, Roud Ghavi, Changouleh Meymeh, Murmuri, Doiraj and Siah Ghav rivers (Ghorbani 2013). Geologically, Ilam Province has various geo-units with complicated background regarding tectonic and seismic activities which is provide sensitive region regarding landslides occurrence. There are several large-scale historical landslides occurred in studied region. One of the largest landslides in the eastern hemisphere and world is believed to have occurred in Ilam Province, more specifically, in the Kabir Kuh anticline at Gorz-e Langar in Darreh Shahr County. According to Harrison & Falcon (1938), the Seymareh landslide moved as much as 30 km^3 of rock as far as 14 km. It is suspected that an earthquake could have triggered such a large landslide (Delchiaro et al. 2020). Figure 2 provide the geological map of the studied region (GSI 2009).

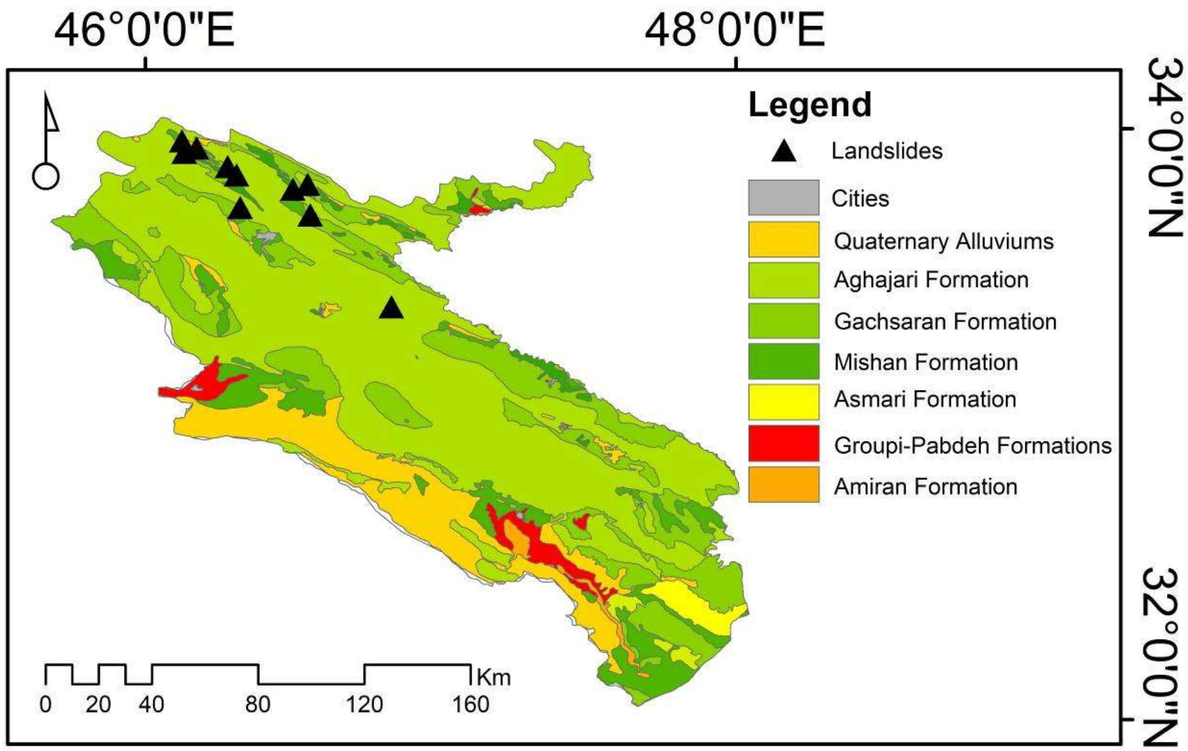

Figure 2: Geological map of the Ilam province.

5. Method and Materials

Multiple-Criteria Decision-Making (MCDM) explicitly evaluates multiple conflicting criteria in decision making which is considered as basics of operational research discipline that deals with the analytical methods' application to improve decision-making process under multiple tasks or extended variables. The structuring of multi-criteria decision and planning is the focus of MCDM which supporting decision-makers in the face of problems as aim of the application (Kumar et al. 2017). Typically, there does not exist a unique optimal solution for decision-based problems and it is necessary to use decision-makers' preferences to differentiate between solutions. Generally, decision-making necessitate is assisted with numerous potential factors were used to solve problems. Better decisions can be made if the influencing factors are given the right amount of priority. If the best weights are given, multi-criteria analysis (which includes a list of potential factors) will produce the best results.

AHP is one of the most efficient MCDM procedures that used in landslide susceptibility assessments. Saaty (1980) proposed the structure-based decision-making technique known as AHP, which relies on a straightforward mathematical model to solve difficult decision-making issues. The ability of AHP to assign the best weights to input triggering factors and produce suitable results, such as landslide susceptibility mapping, has been recognized by worldwide researchers (Cengiz & Ercanoglu 2022, Das et al. 2022). AHP concept in landslide susceptibility analysis is based on importance rate of triggering factors in relation to each other according a scale.

This method gives the factors under consideration a fair amount of weighting because of the unique consistency test it uses. Implementation of AHP approaches require to understand hierarchical structure, relative comparison of triggering factors in decision matrix regarding on scale of importance contrary to targets (objectives), calculation of weights for each variable, estimation of consistency vector, consistency index, random consistency index based on Saaty instructions which is presented in Table 1 (Saaty 1994). The AHP calculation was started based on pairwise comparison matrix and finalized by estimation consistency ratio which leads to estimate the consistency index and the average consistency vector for each target based on following steps.

The AHP procedure can be broken down into the following three stages:

Step 1: Identify the issue and the desired solution based on the requirements and targets,

Step 2: Weighted each criteria and sub-criteria based on importance and priority,

Step 3: Create a comparison matrix based on AHP instructions and checking for consistency with consistency index (CI is the consistency index, λ is the largest eigenvalue of the n-order matrix),

$$CI = \frac{\lambda - n}{n - 1} \qquad (1)$$

Step 4: Testing is measured using consistency ratio (CR). If the value of CI is zero (0), this means the matrix is consistent. If the value of CI obtained is greater than 0 (CI>0), then inconsistency limit applied by Saaty (2000) is tested (RI is random consistency index). If the CR of a smaller matrix is 10%, this means that the inconsistency is acceptable,

$$CR = \frac{CI}{RI} \qquad (2)$$

Step 5: Set up triangular fuzzy membership function to cover all uncertainties faced with each criteria and sub-criteria.

Size of matrix (N)	**1**	**2**	**3**	**4**	**5**	**6**	**7**	**8**	**9**	**10**
Random consistency index, RI	0.00	0.00	0.58	0.90	1.12	1.24	1.32	1.41	1.45	1.49
Consistency ratio, CR	0.00	0.00	0.05	0.08	0.1	0.1	0.1	0.1	0.1	0.1

Table 1: Random consistency index values for different matrix size.

The proposed pairwise comparison matrix is rejected and the factors' relative importance is reconsidered if CR exceeds a predetermined threshold. According to Table 1, the assigned weights are deemed reliable and acceptable if CR falls below the threshold. After reaching the acceptable rate, the data can be converted into the information layers which is used in Geographic Information System (GIS) to generate the landslide susceptibility maps. In this study, ArcGIS 10.4, was used for the entire analysis. Figure 3 provide the process flowchart regarding AHP-MCDM based susceptibility mapping for landslides. As seen in this figure, the landslide susceptibility assessment is classified in several stages was done to provide the zonation maps which can be summarized as following phases.

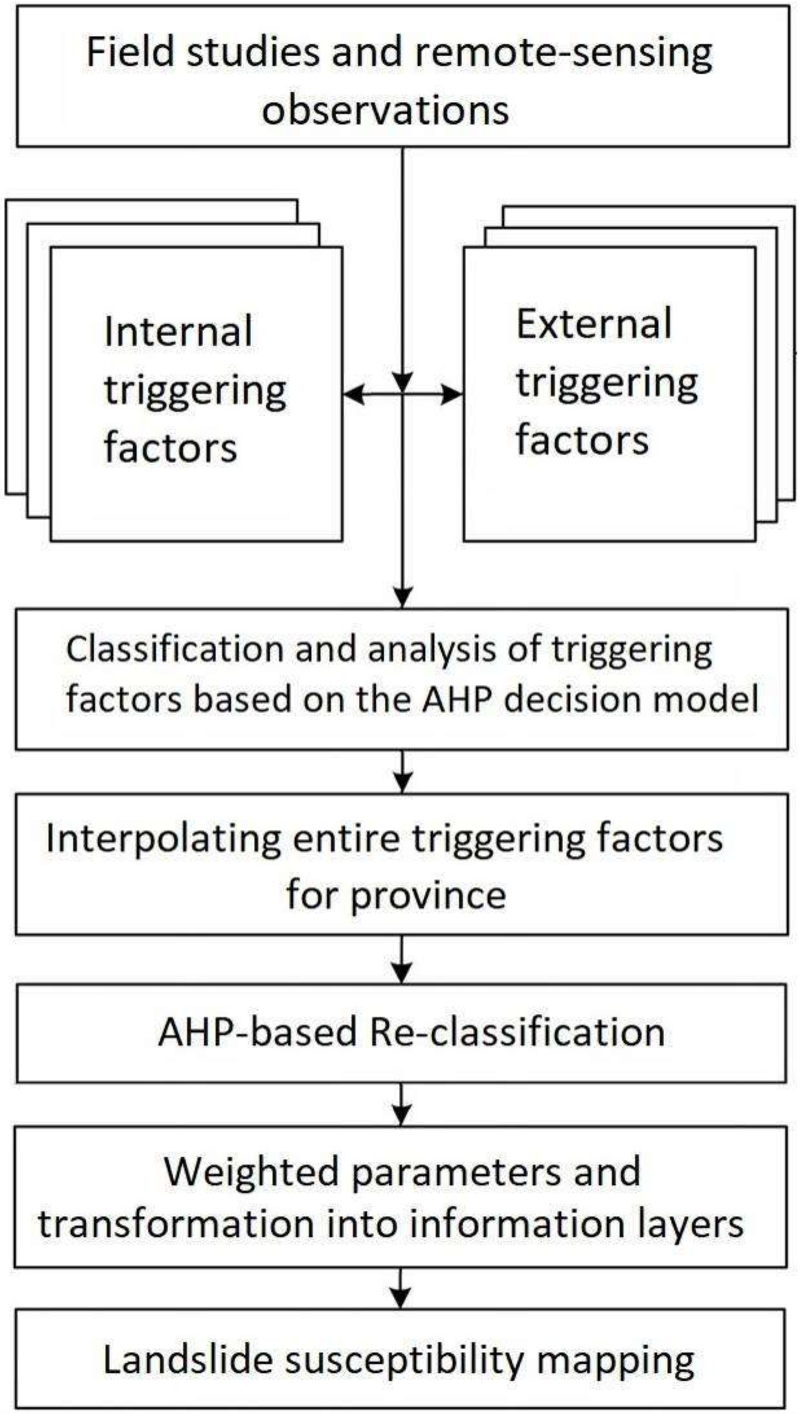

Figure 3: The process flowchart for susceptibility assessment in this article.

5.1. Triggering factors

After a comprehensive field and remote-sensing investigations on Ilam province, fifteen landslide triggering factors are detected for this study. The triggering factors that identified in studied region is presented in Table 2 which is classified as geomorphological, geological, climatological, seismical, and human works. These triggering factors is categorised as internal and external triggering factors. In some literature studies, several historical landslides motioned for the studied region which take them as prone areas regarding landslide occurrence sites (Arekhi & Nazari 2008, Afsari et al. 2014, Rostami et al. 2016, Ahmadi et al. 2021, Ahmadi-Molaverdi et al. 2022). Using these historical landslides which is totally reached on 10 event; as validation to control the results of the landsides susceptibility assessment. Location of these historical landslides was presented in Figure 1. By conducting the remote-sensing observations on historical landslides locations with high-resolution satellite images, the landslides can be identified by surface trace of tension cracks and breaks vegetated area regarding ground movements.

A Digital Elevation Model (DEM) data was used to estimate the elevation and topographic mapping for studied location that used to extract the geomorphologic parameters with resolution about ± 30 m. By using DEM data, the elevation, slope aspect, slope angle, and Compound Topographic Index (CTI) were calculated. Geological map is created by using various ground and remote-sensing data were provided form GSI (https://gsi.ir), Iran Water Resources Management Company, IWRM (https://www.wrm.ir), International Institute of Earthquake Engineering and Seismology, IIEES (http://www.iiees.ac.ir), and Landsat enhanced thematic mapper satellite images, $TM8/ETM^{+}$ (https://earthexplorer.usgs.gov). These data was used to calculate the lithology, Normalized Difference Vegetation Index (NDVI), distance to river, Stream Power Index (SPI), Terrain Ruggedness Index (TRI), and weathering of Ilam province. The CTI, NDVI, and SPI, can be calculated by using following equations:

$$CTI = \ln \frac{a}{\tan b} \quad (3)$$

$$NDVI = \frac{RI - R}{RI + R} \quad (4)$$

$$SPI = \ln(CA \cdot \tan G) \quad (5)$$

where, a is the local upslope area draining through a certain point per unit contour length, tan b is the local slope in radians, RI and R bands are the infrared and red bands of the electromagnetic spectrum, CA and G are catchment area and slope gradient, respectively. The CTR value used to quantify topographic control processes, NDVI value used to interpret vegetation in area, SPI used to measure of the erosive power of flowing water, and TRI indicates how jagged or flat the terrain of a region is on average. Ruggedness is measured in meters of elevation difference for grid points 30 arc-seconds. So, it calculates the difference in elevation values from a center cell and the eight cells immediately surrounding it. Table 3 provide the TRI values for different intervals (Moreno-Ibarra et al. 2011).

Major factors	Sub-factors	Data sources	Resolution
Geomorphologic	Elevation	DEM	± 30 m
	Slope aspect	DEM	± 30 m
	Slope angle	DEM	± 30 m

	Compound topographic index (CTI)	DEM	-
Geologic	Lithology	Geological data	± 30 m
	Vegetation (NDVI)	Landsat TM, ETM$^+$	± 30 m
	Distance to river	DEM, Google Map	± 30 m
	Stream power index (SPI)	IWRM*	-
	Terrain ruggedness index (TRI)	IWRM*	-
	Weathering	Geological data	± 30 m
Climatological	Precipitation	IMO†	± 30 m
Seismic	Distance to faults	GSI, Google Map	± 30 m
	Earthquake distribution	IIEES** data	± 30 m
Human works	Distance to roads	DEM, Google Map	± 30 m
	Distance to cities	DEM, Google Map	± 30 m
Note: *Iran Water Resources Management Company (IWRM); † Iran Meteorological Organization (IMO); ** International Institute of Earthquake Engineering and Seismology (IIEES)			

Table 2: Landslide triggering parameters and data source.

TRI	Interval (m)	Tag	Represents
1	0 – 80	LTS	Level terrain surface
2	81 – 116	NLS	Nearly level surface
3	117 – 161	SRS	Slightly rugged surface
4	162 – 239	IRS	Intermediately rugged surface
5	240 – 497	MRS	Moderately rugged surface
6	498 – 958	HRS	High rugged surface
7	959 – 4367	ERS	Extremely rugged surface

Table 3: TRI values variation.

Climatological data that used in this study, is provided from Iran Meteorological Organization (IMO) which is prepared from the Ilam city meteorological station (https://www.ilammet.ir) were used to create the precipitation layer of information in GIS and a target class in AHP analysis. As known, the precipitation and seismicity is the main triggering factors that highlighted by various scholars. High-intensity rainfall or concentrated seismic activities and earthquakes are the global reasons for activation of land sliding in different scales. So, considering these parameters as high propriety is logically accepted to assessment the landslide susceptibility as same as this article. After preparation of the section for different triggering factors that have impact on landslides occurrence in studied province, these factors are used in AHP decision matrix and entered in GIS to prepare the hazard map of the studied area.

5.2. Application of AHP process model

To investigate the landslide susceptibility of Ilam province, several triggering factors are selected which is included elevation, slope aspect, slope angle, CTI, lithology, NDVI, distance to river, SPI, TRI, weathering, precipitation, distance to faults, earthquake distribution, distance to roads, and distance to cities. These triggering factors' weight and rating values must be known for the landslide susceptibility analysis. Figure 4 is illustrated the triggering factors raster maps that provided in GIS environment. In terms of estimation of weight value for each triggering factor, AHP pairwise comparison matrix had to be built and scored based on Table 4 ((Saaty 2000)). Also, Table 5 provide the consistency requirements that estimated for each triggering factors to validate the decision matrix applicability. After giving weight values to all classes in comparison matrix, the triggering factors which is presented in Table 6, the landslide susceptibility index was calculated according to the Eq. 6.

$$\text{Landslide Suceptibil ity Index} = \sum_{i=1}^{M} X_{ij} \times U_i \qquad (6)$$

where, X_{ij} is the weight of class i in parameter j, U_i is the weight of parameter i, and M is the number of parameters. The results of the landslide susceptibility index calculation will used to develop the landslide susceptibility maps for studied region.

Intensity class	Importance level	Description
1	Equal priority	Two activities contribute equally
3	Low priority	A activity slightly favour one over another
5	Essential priority	A activity highly favour one over another
7	Demonstrated priority	A activity strongly favoured one over another
9	Absolute priority	A activity favourers one over another
2, 4, 6, 8	Intermediate values between the two adjacent judgments	

Table 4: The pairwise comparison matrix scoring system.

Triggering factors	N	λ_{max}	CI	RI	CR
Elevation	3	0.8325	0.0325	0.58	0.0562
Slope aspect	9	0.7670	0.1365	1.45	0.0942
Slope angle	4	0.7926	0.0684	0.90	0.0761
CTI	3	0.8040	0.0305	0.58	0.0527
Lithology	7	0.8977	0.1271	1.32	0.0963
NDVI	4	0.7710	0.0730	0.90	0.0812
Distance to river	4	0.8159	0.0706	0.90	0.0785
SPI	4	0.7012	0.0668	0.90	0.0743
TRI	3	0.8097	0.0305	0.58	0.0526
Weathering	4	0.7216	0.0686	0.90	0.0763
Precipitation	3	0.8724	0.0309	0.58	0.0534

Distance to faults	4	0.7530	0.0681	0.90	0.0757
Earthquake distribution	3	0.8631	0.0296	0.58	0.0512
Distance to roads	4	0.8544	0.0727	0.90	0.0808
Distance to cities	4	0.7710	0.0686	0.90	0.0763

Table 5: The consistency requirements for various triggering factors.

Triggering factors	Matrix class	X_{ij}	U_i
Elevation	< 920 m	0.436	0.43
	921 – 1840 m	0.379	0.38
	1840 m <	0.185	0.19
Slope aspect	Flat	0.107	0.10
	North	0.113	0.12
	Northeast	0.124	0.12
	East	0.100	0.10
	Southeast	0.100	0.10
	South	0.095	0.10
	Southwest	0.121	0.12
	West	0.117	0.12
	Northwest	0.123	0.12
Slope angle	< 5°	0.259	0.25
	5° – 25°	0.248	0.25
	25° – 50°	0.267	0.27
	50° <	0.226	0.23
CTI	0 – 10	0.375	0.37
	10 – 20	0.311	0.32
	20 – 30	0.314	0.31
Lithology	Unit 1	0.143	0.145
	Unit 2	0.137	0.14
	Unit 3	0.142	0.14
	Unit 4	0.145	0.145
	Unit 5	0.144	0.14
	Unit 6	0.130	0.13
	Unit 7	0.159	0.16
NDVI	< 0.1	0.258	0.26
	0.1 – 0.3	0.232	0.23
	0.3 – 0.5	0.260	0.26
	0.5 <	0.250	0.25
Distance to river	< 1500	0.271	0.27
	1500 – 3000	0.235	0.24

	3000 – 4500	0.221	0.22
	4500 <	0.254	0.26
SPI	< -1.5	0.263	0.26
	-1.5 – 2.0	0.263	0.26
	2.0 – 5.5	0.254	0.25
	5.5 <	0.229	0.23
TRI	< 11.5	0.350	0.35
	11.5 – 23	0.320	0.32
	23 <	0.330	0.33
Weathering	< 75	0.254	0.25
	75 – 150	0.239	0.24
	150 – 225	0.262	0.26
	225 <	0.245	0.25
Precipitation	< 600	0.370	0.37
	600 – 700	0.310	0.31
	700 <	0.320	0.32
Distance to faults	< 17,500	0.246	0.25
	17,500 – 35,000	0.274	0.27
	35,000 – 52,500	0.233	0.23
	52,500 <	0.247	0.25
Earthquake distribution	Low density	0.270	0.27
	Moderate density	0.344	0.35
	High density	0.386	0.38
Distance to roads	< 158305	0.246	0.25
	158,305 – 316,610	0.225	0.22
	316,610 – 474,915	0.301	0.30
	474,915 <	0.228	0.23
Distance to cities	< 17,500	0.269	0.27
	17,500 – 35,000	0.255	0.25
	35,000 – 52,500	0.237	0.24
	52,500 <	0.239	0.24

Table 6: The weight triggering factor results in decision matrix by AHP model.

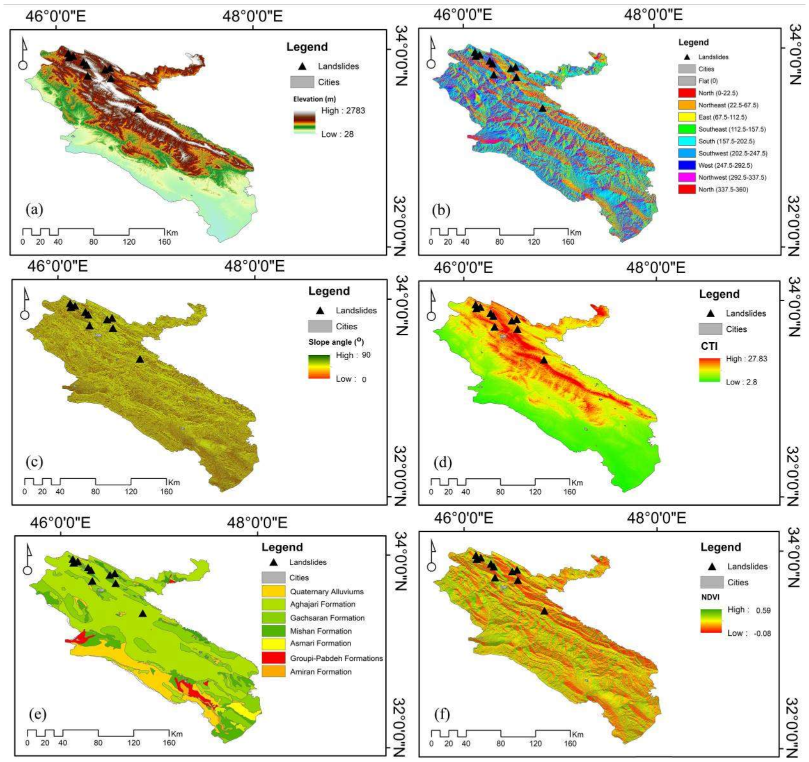
46°0'0"E
48°0'0"E
34°0'0"N
32°0'0"N
Legend
Landslides
Cities
Elevation (m)
High : 2783
Low : 28
(a)
Flat (0)
North (0-22.5)
Northeast (22.5-67.5)
East (67.5-112.5)
Southeast (112.5-157.5)
South (157.5-202.5)
Southwest (202.5-247.5)
West (247.5-292.5)
Northwest (292.5-337.5)
North (337.5-360)
(b)
Slope angle (°)
High : 90
Low : 0
(c)
CTI
High : 27.83
Low : 2.8
(d)
Quaternary Alluviums
Aghajari Formation
Gachsaran Formation
Mishan Formation
Asmari Formation
Groupi-Pabdeh Formations
Amiran Formation
(e)
NDVI
High : 0.59
Low : -0.08
(f)
0 20 40 80 120 160
Km

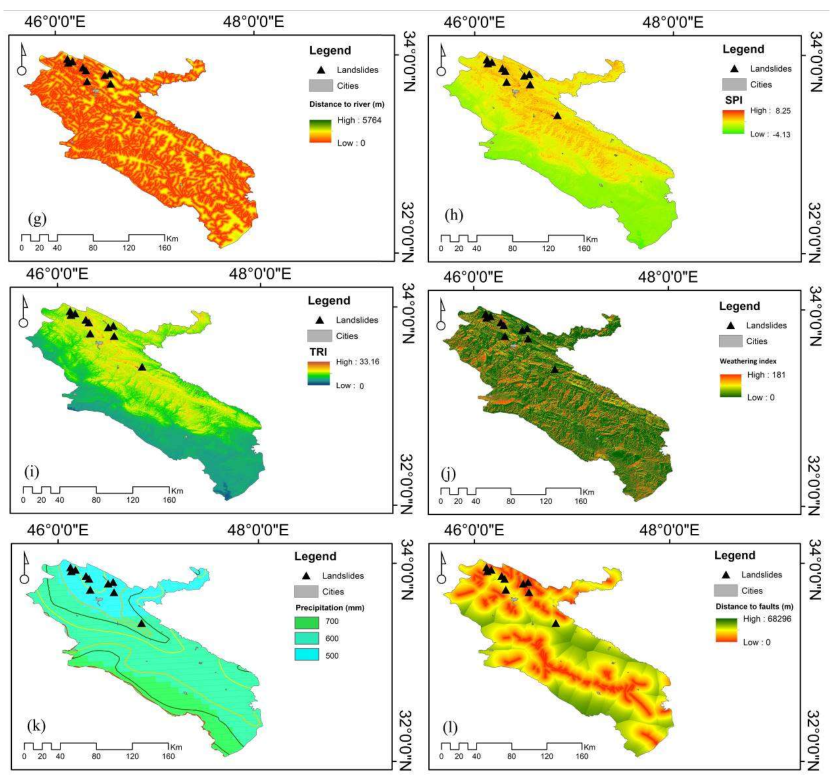
46°0'0"E
48°0'0"E
34°0'0"N
32°0'0"N
Legend
Landslides
Cities
Distance to river (m)
High : 5764
Low : 0
(g)
SPI
High : 8.25
Low : -4.13
(h)
TRI
High : 33.16
Low : 0
(i)
Weathering index
High : 181
Low : 0
(j)
Precipitation (mm)
700
600
500
(k)
Distance to faults (m)
High : 68296
Low : 0
(l)
0 20 40 80 120 160
Km

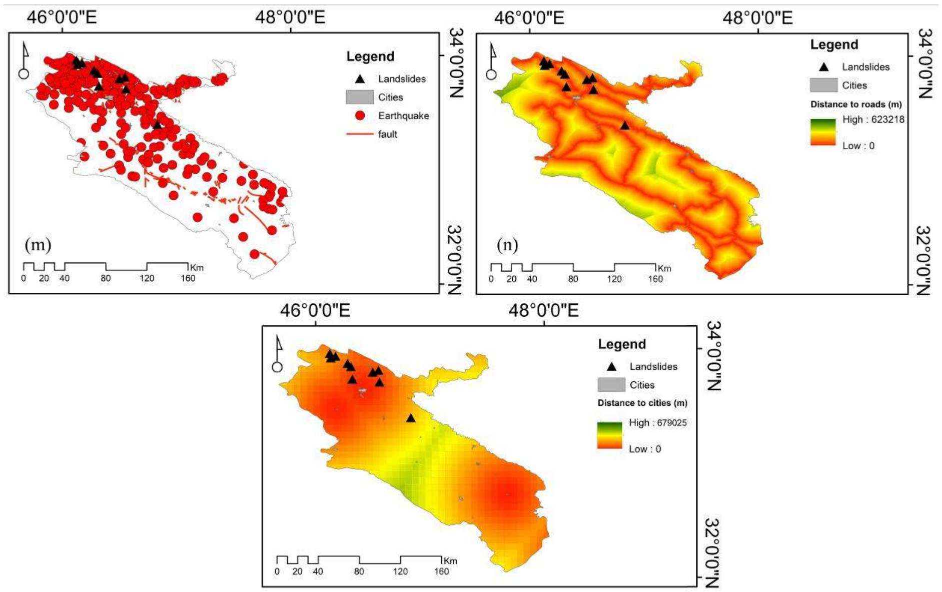

Figure 4: The map of landslide triggering factors prepared for this study: (a) elevation, (b) slope aspect, (c) slope angle, (d) CTI, (e) lithology, (f) NDVI, (g) distance to river, (h) SPI, (i) TRI, (j) weathering, (k) precipitation, (l) distance to faults, (m) earthquake distribution, (n) distance to roads, (o) distance to cities.

6. Results and Discussion

By conducting the results of the spatial analyst / zonal histogram function in ArcGIS program, the relationship between susceptibility zones and percent of historical landslides are estimated and presented in Table 7 which is used as verification. According to the results of the susceptibility analysis for five susceptibility classes included very low (12.5%), low (19.21%), moderate (25.49%), high (27.27%), and very high (15.53%) were validated as very low (9.13%), low (15.01%), moderate (25.03%), high (33.00%), and very high (17.83%). The percentages of the estimation and validation in high and very high susceptibility classes is 42.80% and 50.83%, respectively. The AHP results indicated that the results have proper agreement with the validations which could be used with appropriate reliability in susceptibility assessments. Figure 5 is presented the landslide susceptibility classification map which is provide for Ilam province. The generated results are congruent to that the most area is in moderate to high risk regarding landslides occurrence. But the northwest part of the province is located in very high-risk zone. So, considering the results, decision-makers should conduct relevant investigations on landslide before planning or developments in high-risk areas at Ilam province.

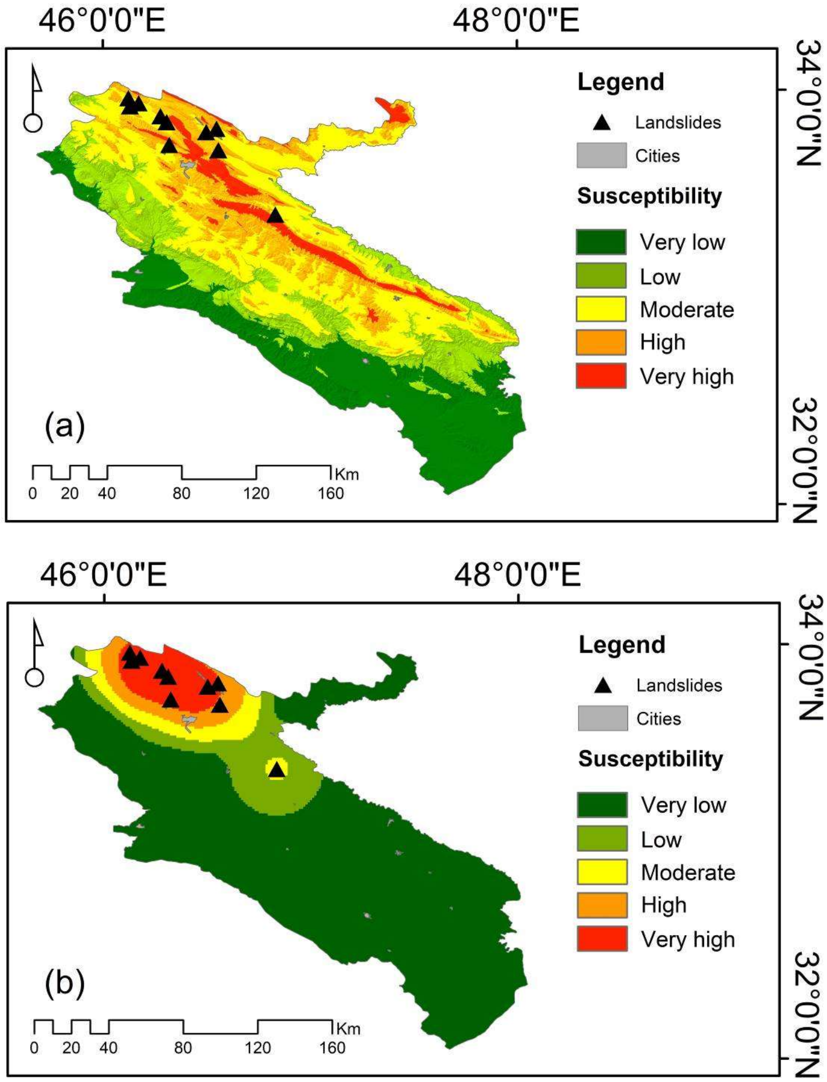

Figure 5: Landslide susceptibility for studied province: (a) estimation map, (b) validation map.

Susceptible class	Estimation (normalized)		Validation (normalized)	
	Pixels	Percentage	Pixels	Percentage
Very low (VL)	912	12.5	835	9.13
Low (L)	1,247	19.21	1,104	15.01
Moderate (M)	1,277	25.49	1,363	25.03
High (H)	1,398	27.27	1,445	33.00
Very high (VH)	1,139	15.53	1,293	17.83
Sum of H + VH	3,835	42.80	2,738	50.83

Table 7: The AHP model verification with historical landslides data.

7. Conclusion

Presented article attempted to provide a susceptibility assessment and hazard zonation map for Ilam province located in western part of Iran. The susceptibility assessment was conducted by using AHP procedure which known as one of the efficient MCDM methodologies. The applied model was implemented on comprehensive decision matrix that composed of fifteen landslide triggering factors which classified as geomorphology (sub-factors: elevation, slope aspect, slope angle, CTI), geological (sub-factors: lithology, NDVI, distance to river, SPT, TRI, weathering), climatological (sub-factor: precipitation), seismical (sub-factors: distance to faults, earthquake distribution), and human works (sub-factors: distance to roads, distance to cities) groups. These triggering factors was selected based on both ground survey and remote-sensing observations which is verified by 10 historical landslides that recorded in studied region. The susceptibility analysis results were used for five-class evaluation is illustrated that the region has 12.5% very low, 19.21% low, 25.49% moderate, 27.27% high, and 15.53% very high which is validated as 9.13% very low, 15.01% low, 25.03% moderate, 33.00% high, and 17.83% very high. The percentages of the estimation in high and very high susceptibility classes are 42.80% and for validation is 50.83% which indicated that AHP model capable to provide reliable and appropriate results. Regarding the susceptibility map of studied region, it appeared that the most area is in moderate to high risk regarding landslides occurrence. But the northwest part of the province is located in very high-risk zone. So, considering the results, decision-makers should conduct relevant investigations on landslide before planning or developments in high-risk areas at Ilam province.

Funding
This research was funded by the National Nature Sciences Foundation of China with Grant No. 42250410321.

References

1. Abedini M., Tulabi S., 2018. Assessing LNRF, FR, and AHP models in landslide susceptibility mapping index: a comparative study of Nojian watershed in Lorestan province, Iran. Environmental Earth Sciences 77(11): 405.
2. Abedini M., Ghasemyan B., Rezaei Mogaddam M.H., 2017. Landslide susceptibility mapping in Bijar city, Kurdistan Province, Iran: a comparative study by logistic regression and AHP models. Environmental Earth Sciences 76(8): 308.
3. Afsari S., Yazdi M., Bahrami A., Carnevale G., 2014. A new deep-sea hatchetfish (Teleostei: Stomiiformes: Sternoptychidae) from the Eocene of Ilam, Zagros Basin, Iran. Bollettino della Società Paleontologica Italiana 53(1): 28.
4. Aghanabati A., 2009. Geology of Iran. Geological Survey and Mineral Exploration of Iran press 708 p.
5. Ahmadi M., Mokhtari D., Khodadadi M., Shahabi H., 2021. Geodiversity evaluation and geoconservation using grid analysis: case study, north of Ilam Province. Applied Geomatics 13(4): 537-553.
6. Ahmadi-Molaverdi M., Jabbari I., Fathnia A., 2022. Geomorphological and Spatial Analysis of Dust sources in Ilam Province, Iran. Sedimentary Geology 436: 106168.

7. Akgun A., Türk N., 2010. Landslide susceptibility mapping for Ayvalik (Western Turkey) and its vicinity by multicriteria decision analysis. Environmental Earth Sciences 61(3): 595-611.
8. Arekhi S., Nazari R. 2008. Zoning erosion intensity and sediment yield using MPSIAC in GIS (Case study: Ilam catchment). Iranian Water Researches Journal 2(2): 77-81.
9. Aslam B., Maqsoom A., Khalil U., Ghorbanzadeh O., Blaschke T., Farooq D., 2022. Evaluation of different landslide susceptibility models for a local scale in the Chitral District, Northern Pakistan. Sensors 22(9): 3107.
10. Azarafza M., Azarafza M., Akgün H., Atkinson P.M., Derakhshani R., 2021. Deep learning-based landslide susceptibility mapping. Scientific Reports 11(1): 24112.
11. Azarafza M., Ghazifard A., Akgün H., Asghari-Kaljahi E., 2018. Landslide susceptibility assessment of South Pars Special Zone, southwest Iran. Environmental Earth Sciences 77(24): 805.
12. Bahrami Y., Hassani H., Maghsoudi A., 2021. Landslide susceptibility mapping using AHP and fuzzy methods in the Gilan province, Iran. GeoJournal 86(4): 1797-1816.
13. Bragagnolo L., da Silva R.V., Grzybowski J.M.V., 2020. Landslide susceptibility mapping with r. landslide: A free open-source GIS-integrated tool based on artificial neural networks. Environmental Modelling & Software 123: 104565.
14. Cengiz L.D., Ercanoglu M., 2022. A novel data-driven approach to pairwise comparisons in AHP using fuzzy relations and matrices for landslide susceptibility assessments. Environmental Earth Sciences 81(7): 222.
15. Chen W., Zhang S., Li R., Shahabi H., 2018. Performance evaluation of the GIS-based data mining techniques of best-first decision tree, random forest, and naïve Bayes tree for landslide susceptibility modeling. Science of the Total Environment 644: 1006-1018.
16. Das S., Sarkar S., Kanungo D.P., 2022. GIS-based landslide susceptibility zonation mapping using the analytic hierarchy process (AHP) method in parts of Kalimpong Region of Darjeeling Himalaya. Environmental Monitoring and Assessment 194(3): 234.
17. Delchiaro M., Rouhi J., Della Seta, M., Martino, S., Nozaem R., Dehbozorgi M., 2020. The Giant Seymareh Landslide (Zagros Mts., Iran): A Lesson for Evaluating Multi-temporal Hazard Scenarios. Applied Geology, Cham: Springer International Publishing, pp. 209-225.
18. Devara M., Tiwari A., Dwivedi R., 2021. Landslide susceptibility mapping using MT-InSAR and AHP enabled GIS-based multi-criteria decision analysis. Geomatics, Natural Hazards and Risk 12(1): 675-693.
19. El-Jazouli A., Barakat A., Khellouk R., 2019. GIS-multicriteria evaluation using AHP for landslide susceptibility mapping in Oum Er Rbia high basin (Morocco). Geoenvironmental Disasters 6(1): 3.
20. Froude M.J., Petley D.N., 2018. Global fatal landslide occurrence from 2004 to 2016. Natural Hazards and Earth System Sciences 18(8): 2161-2181.

21. Geological Survey and Mineral Exploration of Iran, GSI, 2009. Ilam proviance geological map. Geological Survey and Mineral Exploration of Iran press.
22. Ghorbani M., 2013. A summary of geology of Iran. In The economic geology of Iran (pp. 45-64). Springer, Dordrecht.
23. Harrison J.V., Falcon N.L., 1938. An Ancient Landslip at Saidmarreh in Southwestern Iran. The Journal of Geology 46(3): 296-309.
24. He H., Hu D., Sun Q., Zhu L., Liu Y., 2019. A landslide susceptibility assessment method based on GIS technology and an AHP-weighted information content method: A case study of southern Anhui, China. ISPRS International Journal of Geo-information 8(6): 266.
25. Himan S., Saeed K., Baharin A., Mazlan H., 2014. Landslide susceptibility mapping at central Zab basin, Iran: A comparison between analytical hierarchy process, frequency ratio and logistic regression models. Catena 115: 55-70.
26. Hong H., Naghibi S.A., Pourghasemi H.R., Pradhan B., 2016. GIS-based landslide spatial modeling in Ganzhou City, China. Arabian Journal of Geosciences 9 (2): 112.
27. Huang F., Cao Z., Guo J., Jiang S.H., Li S., Guo Z., 2020. Comparisons of heuristic, general statistical and machine learning models for landslide susceptibility prediction and mapping. Catena 191: 104580.
28. International Institute of Earthquake Engineering and Seismology, IIEES, 2022. Earthquake distribution catalogue for Ilam station. Iranian Institute of Earthquake Engineering and Seismology, Tehran, Iran.
29. Jam A.S., Mosaffaie J., Sarfaraz F., Shadfar S., Akhtari R., 2021. GIS-based landslide susceptibility mapping using hybrid MCDM models. Natural Hazards 108(1): 1025-1046.
30. Kayastha P., Dhital M.R., De Smedt F., 2013. Application of the analytical hierarchy process (AHP) for landslide susceptibility mapping: A case study from the Tinau watershed, west Nepal. Computers & Geosciences 52: 398-408.
31. Khalil U., Imtiaz I., Aslam B., Ullah I., Tariq A., Qin S., 2022. Comparative analysis of machine learning and multi-criteria decision making techniques for landslide susceptibility mapping of Muzaffarabad district. Frontiers in Environmental Science 10: 1-19.
32. Khezri S., 2011. Landslide susceptibility in the Zab Basin, northwest of Iran. Procedia-Social and Behavioral Sciences 19: 726-731.
33. Kritikos T.R., Davies T.R., 2011. GIS-based multi-criteria decision analysis for landslide susceptibility mapping at northern Evia, Greece. Zeitschrift der Deutschen Gesellschaft für Geowissenschaften 62(4):421-434.
34. Kumar A., Sah B., Singh A.R., Deng Y., He X., Kumar P., Bansal R.C., 2017. A review of multi criteria decision making (MCDM) towards sustainable renewable energy development. Renewable and Sustainable Energy Reviews 69: 596-609.
35. Kumar R., Anbalagan R., 2016. Landslide susceptibility mapping using analytical hierarchy process (AHP) in Tehri reservoir rim region, Uttarakhand. Journal of the Geological Society of India 87(3): 271-286.

36. Mandal B., Mandal S., 2018. Analytical hierarchy process (AHP) based landslide susceptibility mapping of Lish river basin of eastern Darjeeling Himalaya, India. Advances in Space Research 62(11): 3114-3132.
37. Mansouri Daneshvar M.R., 2014. Landslide susceptibility zonation using analytical hierarchy process and GIS for the Bojnurd region, northeast of Iran. Landslides 11(6): 1079-1091.
38. Maqsoom A., Aslam B., Khalil U., Kazmi Z.A., Azam S., Mehmood T., 2021. Landslide susceptibility mapping along the China Pakistan Economic Corridor (CPEC) route using multi-criteria decision-making method. Model. Earth Systems and Environment 8: 1519-1533.
39. Mohammady M., Morady H.R., Feiz Nia S., Pourghasemi H.R., 2010. Prioritization of Landslide Effective Factors and it´ s Hazard Mapping using Information Value and AHP Models (Case Study: A Part of Haraz Watershed). Scientific Quarterly Journal of Geosciences 19(74): 27-32.
40. Moradi M., Bazyar M.H., Mohammadi Z., 2012. GIS-based landslide susceptibility mapping by AHP method, a case study, Dena City, Iran. Journal of Basic and Applied Scientific Research 2(7): 6715-6723.
41. Moreno-Ibarra M., Torres M., Quintero R., Guzman G., Menchaca-Mendez R., 2011. Semantic assessment of similarity between raster elevation datasets. Revista Facultad de Ingeniería Universidad de Antioquia (59): 37-46.
42. Mousavi S.M., Ataie-Ashtiani B., Hosseini S.M., 2022. Comparison of statistical and MCDM approaches for flood susceptibility mapping in northern Iran. Journal of Hydrology 612: 128072.
43. Myronidis D., Papageorgiou C., Theophanous S., 2016. Landslide susceptibility mapping based on landslide history and analytic hierarchy process (AHP). Natural Hazards 81(1): 245-263.
44. Nanehkaran Y.A., Mao Y., Azarafza M., Kockar M.K., Zhu H.H., 2021. Fuzzy-based multiple decision method for landslide susceptibility and hazard assessment: A case study of Tabriz, Iran. Geomechanics and Engineering 24(5): 407-418.
45. Nguyen T.T.N., Liu C.C., 2019. A new approach using AHP to generate landslide susceptibility maps in the Chen-Yu-Lan Watershed, Taiwan. Sensors 19(3): 505.
46. Nikoobakht S., Azarafza M., Akgün H., Derakhshani R., 2022. Landslide Susceptibility Assessment by Using Convolutional Neural Network. Applied Sciences 12(12): 5992.
47. Panchal S., Shrivastava A.K., 2020. Application of analytic hierarchy process in landslide susceptibility mapping at regional scale in GIS environment. Journal of Statistics and Management Systems 23(2): 199-206.
48. Pourghasemi H.R., Rossi M., 2017. Landslide susceptibility modeling in a landslide prone area in Mazandarn Province, north of Iran: a comparison between GLM, GAM, MARS, and M-AHP methods. Theoretical and Applied Climatology 130(1): 609-633.

49. Pourghasemi H.R., Pradhan B., Gokceoglu C., 2012. Application of fuzzy logic and analytical hierarchy process (AHP) to landslide susceptibility mapping at Haraz watershed, Iran. Natural Hazards 63(2): 965-996.
50. Roodposhti M.S., Rahimi S., Beglou M.J., 2014. PROMETHEE II and fuzzy AHP: an enhanced GIS-based landslide susceptibility mapping. Natural Hazards 73(1): 77-95.
51. Rostami Z.A., Al-Modaresi S.A., Fathizad H., Faramarzi M., 2016. Landslide susceptibility mapping by using fuzzy logic: a case study of Cham-gardalan catchment, Ilam, Iran. Arabian Journal of Geosciences 9(17): 1-11.
52. Roy D., Das S., Mitra R., 2022. An application of geospatial-based multi-criteria decision-making technique to identify landslide susceptibility zones in the Ragnu Khola River Basin of Darjeeling Himalayan region, India. Applied Geomatics 14(4): 731-749.
53. Rozos D., Bathrellos D.G., Skilodimou D.H., 2010. Landslide Susceptibility Mapping Of The Northeastern Part of Achaia Prefectureusing Analytical Hierarchical Process and GIS Techniques. Bulletin of the Geological Society of Greece 43(3): 1637-1646.
54. Saaty T.L., 2000. Fundamentals of decision making and priority theory 1st Edition. RWS Publications, Pittsburgh, p 477.
55. Saaty T.L., 1980. The analytical hierarchy process, planning, priority. Resource allocation. USA: RWS Publications.
56. Saaty T.L., 1994. How to make a decision: the analytic hierarchy process. Interfaces 24(6): 19-43.
57. Sahin E.K., 2020. Assessing the predictive capability of ensemble tree methods for landslide susceptibility mapping using XGBoost, gradient boosting machine, and random forest. SN Applied Sciences 2(7): 1308.
58. Santacana N., Baeza B., Corominas J., De Paz A., Marturiá J., 2003. A GIS-based multivariate statistical analysis for shallow landslide susceptibility mapping in La Pobla de Lillet area (Eastern Pyrenees, Spain). Natural Hazards 30(3): 281-295.
59. Sur U., Singh P., Meena S.R., 2020. Landslide susceptibility assessment in a lesser Himalayan road corridor (India) applying fuzzy AHP technique and earth-observation data. Geomatics, Natural Hazards and Risk 11(1): 2176-2209.
60. Swetha T.V., Gopinath G., 2020. Landslides susceptibility assessment by analytical network process: a case study for Kuttiyadi river basin (Western Ghats, southern India). SN Applied Sciences 2(11): 1776.
61. Tsangaratos P., Ilia I., 2016. Comparison of a logistic regression and naïve bayes classifier in landslide susceptibility assessments: The influence of models complexity and training dataset size. Catena 145: 164-179.
62. Yalcin A., Reis S., Aydinoglu A.C., Yomralioglu T., 2011. A GIS-based comparative study of frequency ratio, analytical hierarchy process, bivariate statistics and logistics regression methods for landslide susceptibility mapping in Trabzon, NE Turkey. Catena 85(3): 274-287.

63. Yamusa I.B., Ismail M.S., Tella A., 2022. Highway Proneness Appraisal to Landslides along Taiping to Ipoh Segment Malaysia, Using MCDM and GIS Techniques. Sustainability 14(15): 9096.
64. Youssef A.M., 2015. Landslide susceptibility delineation in the Ar-Rayth area, Jizan, Kingdom of Saudi Arabia, using analytical hierarchy process, frequency ratio, and logistic regression models. Environmental Earth Sciences 73(12): 8499-8518.
65. Youssef A.M., Al-Kathery M., Pradhan B., 2015. Landslide susceptibility mapping at Al-Hasher area, Jizan (Saudi Arabia) using GIS-based frequency ratio and index of entropy models. Geosciences Journal 19(1): 113-134.
66. Zêzere J.L., Pereira S., Melo R., Oliveira S.C., Garcia R.A., 2017. Mapping landslide susceptibility using data-driven methods. Science of the Total Environment 589: 250-267.